Article

Hydrogen-Bond Interaction in Organic Conductors: Redox Activation, Molecular Recognition, Structural Regulation, and Proton Transfer in Donor–Acceptor Charge-Transfer Complexes of TTF-Imidazole

Tsuyoshi Murata, Yasushi Morita, Yumi Yakiyama, Kozo Fukui, Hideki Yamochi, Gunzi Saito, and Kazuhiro Nakasuji

J. Am. Chem. Soc., **2007**, 129 (35), 10837-10846• DOI: 10.1021/ja072607m • Publication Date (Web): 14 August 2007

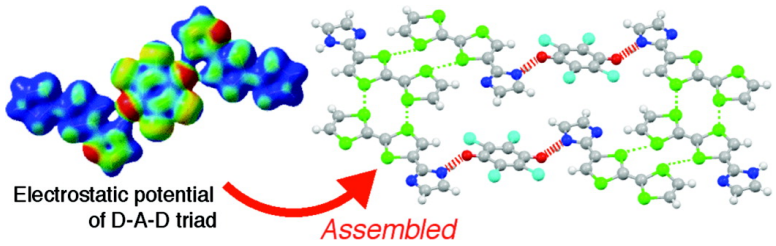

More About This Article

Additional resources and features associated with this article are available within the HTML version:

- Supporting Information
- Links to the 7 articles that cite this article, as of the time of this article download
- Access to high resolution figures
- Links to articles and content related to this article
- Copyright permission to reproduce figures and/or text from this article

View the Full Text HTML

J|A|C|S
ARTICLES
Published on Web 08/14/2007

Hydrogen-Bond Interaction in Organic Conductors: Redox Activation, Molecular Recognition, Structural Regulation, and Proton Transfer in Donor−Acceptor Charge-Transfer Complexes of TTF-Imidazole

Tsuyoshi Murata,[†,‡] Yasushi Morita,*[,†,§] Yumi Yakiyama,[†] Kozo Fukui,[§] Hideki Yamochi,[||] Gunzi Saito,*[,‡,||] and Kazuhiro Nakasuji*[,†,⊥]

Contribution from the Department of Chemistry, Graduate School of Science, Osaka University, Toyonaka, Osaka 560-0043, Japan, Division of Chemistry, Graduate School of Science, Kyoto University, Sakyo-ku, Kyoto 606-8502, Japan, PRESTO, Japan Science and Technology Agency (JST), Kawaguchi, Saitama 332-0012, Japan, Research Center for Low Temperature and Materials Science, Kyoto University, Sakyo-ku, Kyoto 606-8502, Japan, and Fukui University of Technology, Fukui, Fukui 910-8505, Japan

Received April 14, 2007; E-mail: morita@chem.sci.osaka-u.ac.jp; saito@kuchem.kyoto-u.ac.jp; K-nakasuji@fukui-ut.ac.jp

Abstract: Hydrogen-bond interaction in donor−acceptor charge-transfer complexes of TTF-imidazole demonstrated the electronic effects in terms of control of component ratio and redox activation. These unprecedented effects of hydrogen bonds renewed the criteria giving "a high probability of being organic metals" and produced a number of highly conductive complexes with various acceptors having a wide range of electron-accepting ability. In *p*-chloranil complex, both molecules were linked by hydrogen bonds and formed a D−A−D triad, regulating the donor−acceptor composition to be 2:1. Theoretical calculations have revealed that the polarizability of hydrogen bonds controls the redox ability of the donor and *p*-benzoquinone-type acceptors and afforded different ionicity in complexes from those expected by the difference of redox potentials between donor and acceptors. In the *p*-chloranil complex, this electronic and structural regulation by hydrogen bond realized the first metallic donor−acceptor charge-transfer complex based on hydrogen bond functionalized TTF. Hydrogen bonds controlled also molecular arrangements in charge-transfer complexes, giving diverse and highly ordered assembled structures, D−A−D triad in the *p*-chloranil complex, one-dimensional zigzag chain in I_5 salt, alternating donor−acceptor chain in chloranilic acid complex, and D−A−D−A cyclic tetramer in nitranilic acid complex. Furthermore, TTF-imidazole acted as electron donor as well as proton acceptor in anilic acid complexes and realized the simultaneous charge- and proton-transfer complexes. These investigations demonstrated the new and intriguing potentials of the hydrogen bond in the development of organic conductors and multifunctional molecular materials.

Introduction

Charge-transfer (CT) salts and complexes based on tetrathiafulvalene (TTF) and its derivatives have offered a number of conducting and superconducting materials and are still in the center of the research field of molecular conductors.[1] The most essential strategies to design conducting CT salts and complexes are (1) generation of charge carrier and (2) formation of conduction path.[2] The carrier is provided by a radical electron, and the transport barrier is removed by the formation of a partially filled band structure (partial CT state). In the CT salts composed of electron donors and acceptors with redox-inactive counterions, CT degrees are determined by component ratios. However, only a few distinct methodologies, especially a chemical one, to control component ratios have been proposed, where the supramolecular assemblies composed of halide anions and iodine-containing neutral molecules are utilized.[3] In the cases of donor−acceptor CT complexes, not only control of component ratio but also selection of appropriate differences between electron donor and acceptor strengths are widely accepted as a key design criteria to afford partial CT complexes.[4] In the quasi-one-dimensional TTF−TCNQ systems, −0.02 to +0.34 V of difference of the first oxidation and reduction

[†] Osaka University.
[‡] Division of Chemistry, Kyoto University.
[§] PRESTO, JST.
[||] Research Center for Low Temperature and Materials Science, Kyoto University.
[⊥] Fukui University of Technology.

(1) (a) Ishiguro, T.; Yamaji, K.; Saito, G. *Organic Superconductors;* Springer-Verlag: Berlin, 1990. (b) Williams, J. M.; Ferraro, J. R.; Thorn, R. J.; Calson, K. D.; Geiser, U.; Wang, H. H.; Kini, A. M.; Whangbo, M. H. *Organic Superconductors (Including Fullerenes): Synthesis, Structure, Properties, and Theory;* Prentice Hall: Englewood Cliffs, NJ, 1992. (c) *TTF Chemistry: Fundamentals and Applications of Tetrathiafulvalene;* Yamada, J., Sugimoto, T., Eds.; Kodansha: Tokyo, 2004. (d) Saito, G.; Yoshida, Y. *Bull. Chem. Soc. Jpn.* **2007**, *80*, 1−137.

(2) (a) Garito, A. F.; Heeger, A. J. *Acc. Chem. Res.* **1974**, *7*, 232−240. (b) Torrance, J. B. *Acc. Chem. Res.* **1979**, *12*, 79−86.

(3) Yamamoto, H. M.; Kato, R. *Chem. Lett.* **2000**, 970−971.

(4) (a) Torrance, J. B.; Vazquez, J. E.; Mayerle, J. J.; Lee, V. Y. *Phys. Rev. Lett.* **1981**, *46*, 253−257. (b) Saito, G.; Ferraris, J. P. *Bull. Chem. Soc. Jpn.* **1980**, *53*, 2141−2145.

Chart 1. Chemical Structures of Compounds in the Text

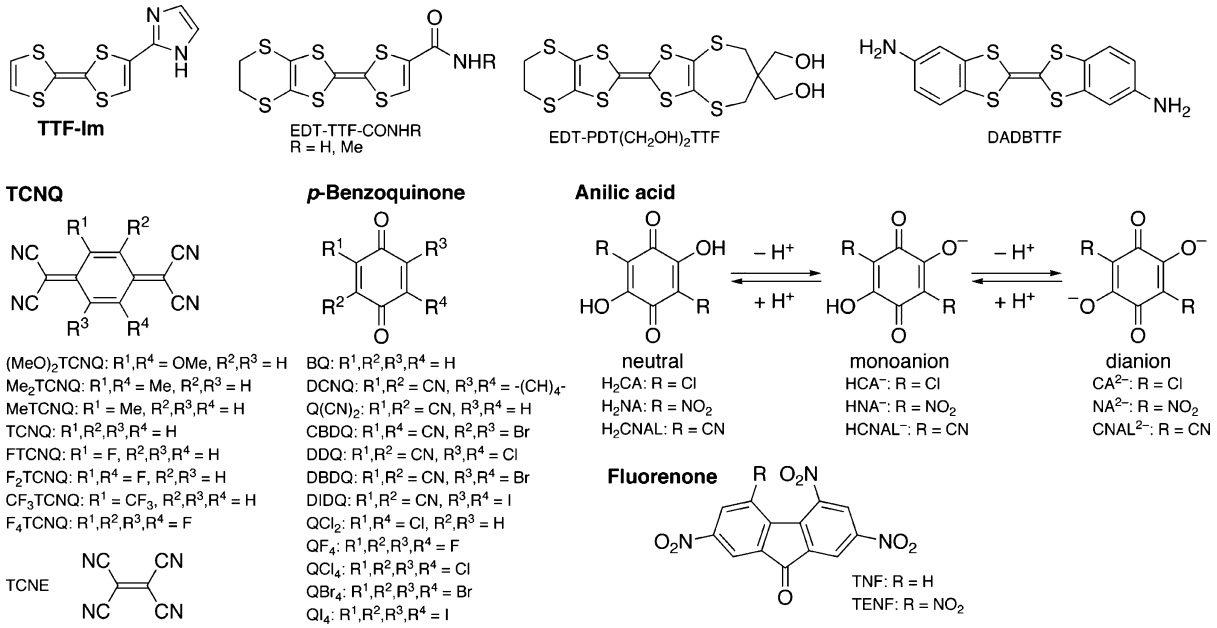

potentials of donors and acceptors (ΔE), respectively, generally gives a crucial factor to obtain highly conductive complexes.[1d,4] This limitation is modulated by increasing self-assembling ability or dimensionality of electronic structure in several electron donor systems having ethylenedioxy group[5] or heavy chalcogen atoms.[6]

The conduction path is established mainly in the segregated structure and by formation of effective intermolecular overlap of π- or d-orbitals.[1] Numerous attempts to control molecular arrangement in CT salts and complexes have been performed by the enhancement of chalcogen atom interactions[1c,d] and by the introduction of halogen or hydrogen bonds (H-bonds).[3,7] Although a number of H-bond functionalized TTF derivatives have been synthesized, most of them gave low conductive or insulating CT salts and complexes.[7] As rare events, the metallic CT salts with inorganic counteranions have been prepared in EDT-TTF-CONHR (R = H or Me)[8] and EDT-PDT(CH_2-$OH)_2$TTF salts (Chart 1).[9] It should be emphasized that no metallic CT complexes based on the H-bond functionalized TTF derivatives with redox active organic electron acceptors are demonstrated before we study (vide infra). The introduction of H-bond interactions is also recognized as a methodology to modulate the redox activity as demonstrated in diaminodibenzo TTF (DADBTTF)[10] and the host−guest TTF systems.[11]

The imidazole ring is an aromatic π-electronic system having two nitrogen atoms as the proton donor/acceptor functionalities and forms strong and directional H-bond interactions. This feature has attracted much attention in crystal engineering, and a number of supramolecular assemblies based on the imidazole system have been formed in the molecule-based magnets[12] and molecular conductors.[13] Furthermore, imidazole is a Brönsted acid and base causing the proton transfer (PT) process, which plays an important role in biological systems such as the redox process of cytochrome *c*.[14] The PT process of imidazole also causes high proton conductivity of imidazole crystal[15] where a one-dimensional chain by N−H···N H-bonds is formed.[16] The complex formation between an electron donor and acceptor having PT ability has demonstrated the complex isomerism between CT and PT types in the aromatic amine−polynitrophenol complexes[17] and the cooperative CT and PT system shown in benzoquinhydrone complexes.[18] These systems have opened a new opportunity in the development of multifunctional molecular materials.[19]

To explore new molecular conductors electronically and structurally modulated by the H-bond, we designed a new TTF

(5) (a) Horiuchi, S.; Yamochi, H.; Saito, G.; Sakaguchi, K.; Kusunoki, M. *J. Am. Chem. Soc.* **1996**, *118*, 8604−8622. (b) Saito, G.; Sasaki, H.; Aoki, T.; Yoshida, Y.; Otsuka, A.; Yamochi, H.; Drozdova, O. O.; Yakushi, K.; Kitagawa, H.; Mitani, T. *J. Mater. Chem.* **2002**, *12*, 1640−1649.
(6) Pac, S.-S.; Saito, G. *J. Solid State Chem.* **2002**, *168*, 486−496.
(7) Fourmigué, M.; Batail, P. *Chem. Rev.* **2004**, *104*, 5379−5418.
(8) (a) Heuzé, K.; Fourmigué, M.; Batail, P.; Canadell, E.; Auban-Senzier, P. *Chem.−Eur. J.* **1999**, *5*, 2971−2976. (b) Heuzé, K.; Mézière, C.; Fourmigué, M.; Batail, P.; Coulon, C.; Canadell, E.; Auban-Senzier, P.; Jérome, D. *Chem. Mater.* **2000**, *12*, 1898−1904. (c) Baudron, S. A.; Batail, P.; Coulon, C.; Clérac, R.; Canadell, E.; Laukhin, V.; Melzi, R.; Wzietek, P.; Jérome, D.; Auban-Senzier, P.; Ravy, S. *J. Am. Chem. Soc.* **2005**, *127*, 11785−11797.
(9) Liu, S.-X.; Neels, A.; Stoeckli-Evans, H.; Pilkington, M.; Wallis, J. D.; Decurtins, S. *Polyhedron* **2004**, *23*, 1185−1189.
(10) Morita, Y.; Miyazaki, E.; Fukui, K.; Maki, S.; Nakasuji, K. *Bull. Chem. Soc. Jpn.* **2005**, *78*, 2014−2018.
(11) Boyd, A. S. F.; Cooke, G.; Duclairoir, F. M. A.; Rotello, V. M. *Tetrahedron Lett.* **2003**, *44*, 303−306.
(12) (a) Yoshioka, N.; Inoue, H. In *Magnetic Properties of Organic Materials;* Lahti, P. M., Ed.; Marcel Dekker: New York, 1999; pp 553−572. (b) Luneau, D.; Rey, P. *Mol. Cryst. Liq. Cryst.* **1995**, *273*, 81−87. (c) Ferrer, J. R.; Lahti, P. M.; George, C.; Antorrena, G.; Palacio, F. *Chem. Mater.* **1999**, *11*, 2205−2210.
(13) (a) Akutagawa, T.; Saito, G.; Kusunoki, M.; Sakaguchi, K. *Bull. Chem. Soc. Jpn.* **1996**, *69*, 2487−2511. (b) Akutagawa, T.; Hasegawa, T.; Nakamura, T.; Inabe, T.; Saito, G. *Chem.−Eur. J.* **2002**, *8*, 4402−4411. (c) Morita, Y.; Murata, T.; Fukui, K.; Yamada, S.; Sato, K.; Shiomi, D.; Takui, T.; Kitagawa, H.; Yamochi, H.; Saito, G.; Nakasuji, K. *J. Org. Chem.* **2005**, *70*, 2739−2744. (d) Murata, T.; Morita, Y.; Nakasuji, K. *Tetrahedron* **2005**, *61*, 6056−6063.
(14) Iwata, S.; Ostermeier, C.; Ludwig, B.; Michel, H. *Nature* **1995**, *376*, 660−669.
(15) Kawada, A.; McGhie, A. R.; Labes, M. M. *J. Chem. Phys.* **1970**, *52*, 3121−3125.
(16) (a) Martinez-Carrera, S. *Acta Crystallogr.* **1966**, *20*, 783−789. (b) Craven, B. M.; McMullan, R. K.; Bell, J. D.; Freeman, H. C. *Acta Crystallogr., Sect. B* **1977**, *33*, 2585−2589.
(17) For examples, see: (a) Saito, G.; Matsunaga, Y. *Bull. Chem. Soc. Jpn.* **1971**, *44*, 3328−3335. (b) Matsunaga, Y.; Saito, G. *Bull. Chem. Soc. Jpn.* **1972**, *45*, 963−964. (c) Saito, G.; Matsunaga, Y. *Bull. Chem. Soc. Jpn.* **1972**, *45*, 2214−2215.
(18) Mitani, T.; Saito, G.; Urayama, H. *Phys. Rev. Lett.* **1988**, *60*, 2299−2302.

Scheme 1. CT and PT Processes of the **TTF-Im** System

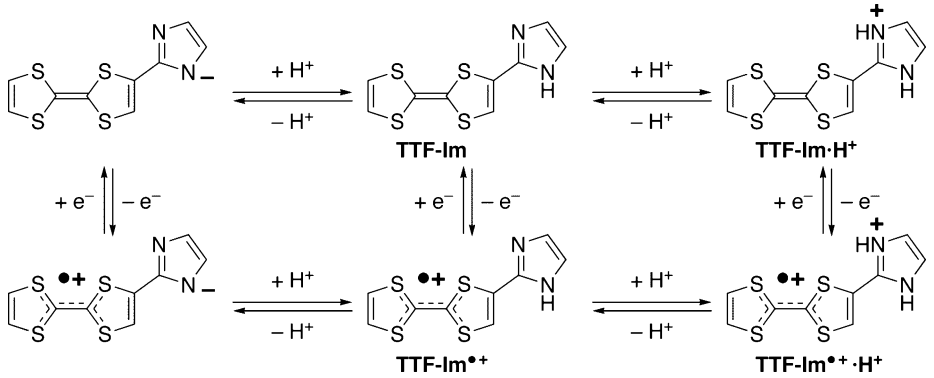

derivative having an imidazole ring, TTF-imidazole (**TTF-Im**).[20] In this article, we have investigated the donor−acceptor CT complexes of **TTF-Im** with TCNQ, *p*-benzoquinone, fluorenone, and anilic acid-type acceptors (Chart 1). Crystal structure analyses and theoretical calculations of the CT complexes revealed the electronic and structural roles of H-bond interaction: (1) control of donor−acceptor ratio on the basis of site-selective molecular recognition, (2) enhancement of redox ability by the high polarizability, and (3) regulation of molecular arrangements in the solid state. The electronic effects (1) and (2) efficiently controlled the ionicity of donor and acceptors and realized partial CT complexes with a wide range of acceptors in the accepting ability and produced highly conductive complexes beyond the criteria concerning ΔE.[1d,4] In the complexes with anilic acid-type acceptors, **TTF-Im** showed simultaneous CT and PT processes (Scheme 1). Taking advantage of these new roles, we emphasize that our studies give new tools for the molecular design of the conductive CT complexes and multifunctional molecular conductors.

Experimental Section

Materials. Preparation of **TTF-Im** was reported in our previous article.[20] Acceptors were purified by sublimation or recrystallization.

Measurements. Infrared (IR) spectra were measured using KBr plates on JASCO FT/IR-660M or Perkin-Elmer Paragon 1000 (resolution 2 or 4 cm^{-1}), and electronic spectra were measured by a Shimadzu UV/vis-NIR scanning spectrophotometer UV-3100 PC. Measurement of Raman spectra was carried out using JASCO NR1800 (resolution ca. 2 cm^{-1}). Elemental analyses were performed at the Graduate School of Science, Osaka University, and the Center for Organic Elemental Microanalysis, Kyoto University. Cyclic voltammetric (CV) measurements were made with an ALS Electrochemical Analyzer model 612A and recorded with a 3-mm-diameter glassy plate carbon electrode and Pt wire counter electrode in DMF containing 0.1 M $Et_4N^+ClO_4^-$ as the supporting electrolyte at room temperature. The experiments employed an $Ag/AgNO_3$ reference electrode. The final results were calibrated with ferrocene/ferrocenium couple (Fc/Fc^+). Direct current electrical conductivity measurements for CT complexes were made on the compressed powder pellets and on single crystal only for **16** by a conventional two- or four-probe method using gold paint and gold wires. The too small or thin size, efflorescent feature, and/or too low conductivity of the other crystal complexes prevented the conductivity measurements on their single crystals.

X-ray Crystallography. X-ray crystallographic measurements were made on a MAC Science MXC$^{\chi}$ automatic four-circle diffractometer for **1**, on a Rigaku Raxis-Rapid imaging plate for **16**, **20**, and **21a**, and on Rigaku Saturn or Mercury CCD area detectors for **22** and **23b**, respectively, with a graphite monochromated Mo Kα ($\lambda = 0.71070$ Å) for **1**, **20**, **21a**, **22**, and **23b** and Cu Kα radiation ($\lambda = 1.54180$ Å) for **16**. Structures were determined by direct method using SHELXS-97 for **1**, **20**, and **21a**,[21a] SIR-97 for **16**, SHELXS-86 for **23b**,[22] and SIR-2002 for **22**. Refinements were performed by full-matrix least-squares on F^2 using SHELXL-97[21b] for **1**, **16**, **20**, **21a**, and **22**, and using the teXsan crystallographic software package for **23b**.[23] All non-hydrogen atoms were refined anisotropically except for the disordered solvent molecules (H_2O) in **22**, and all hydrogen atoms were included but not refined. Empirical (**16** and **22**) and symmetry-related (**20**, **21a**, and **23b**) absorption corrections were applied. Selected crystal data and data collection parameters are given in Table S1 in Supporting Information.

Theoretical Calculations. Density functional theory (DFT) calculations were performed at the RB3LYP/6-31G(d)//RB3LYP/6-31G(d) level on Gaussian 98. The DFT calculations of H-bonded pairs (TTF-Im−MeCN from **1**, **TTF-Im**−QCl_4−**TTF-Im** and Im−QCl_4−Im from **16**) were performed using the structures extracted from the crystal structures. The parameters of non-H-bonded pairs were obtained by the elongation of H-bond distances by 10 Å.

Results and Discussion

In the CV measurement, **TTF-Im** shows the first oxidation potential (E^D) at −0.06 V vs Fc/Fc^+ which is slightly higher than that of TTF (−0.09 V). Preparation of CT complexes was performed by the direct mixing or the diffusion methods with 1:2 to 2:1 molar ratio of **TTF-Im** and acceptors in appropriate solvents (MeCN, CH_2Cl_2, PhCl, and THF). Complexes with weak acceptors, $(MeO)_2TCNQ$, QCl_2, and BQ ($E^A = -0.33$, −0.56, and −0.89 V, respectively), were not obtained. The IR spectra of all CT complexes were interpreted essentially by the superimpositions of the neutral, ionic, and/or PT species of **TTF-Im** and each acceptor. The chemical reaction products were not found in the complexes. All complexes exhibited broad and multiple N−H stretching absorption at around 2500−3500 cm^{-1},

(19) (a) Nakasuji, K.; Sugiura, K.; Kitagawa, T.; Toyoda, J.; Okamoto, H.; Okaniwa, K.; Mitani, T.; Yamamoto, H.; Murata, I.; Kawamoto, A.; Tanaka, J. *J. Am. Chem. Soc.* **1991**, *113*, 1862−1864. (b) Sugiura, K.; Toyoda, J.; Okamoto, H.; Okaniwa, K.; Mitani, T.; Kawamoto, A.; Tanaka, J.; Nakasuji, K. *Angew. Chem., Int. Ed. Engl.* **1992**, *31*, 852−854. (c) Kubo, T.; Ohashi, M.; Miyazaki, K.; Ichimura, A.; Nakasuji, K. *Inorg. Chem.* **2004**, *43*, 7301−7307.

(20) Murata, T.; Morita, Y.; Fukui, K.; Sato, K.; Shiomi, D.; Takui, T.; Maesato, M.; Yamochi, H.; Saito, G.; Nakasuji, K. *Angew. Chem., Int. Ed.* **2004**, *43*, 6343−6346. Magnetic properties and band calculation of the QCl_4 complex **16** are mentioned.

(21) (a) Sheldrick, G. M. *SHELXS-97, Program for the Solution of Crystal Structures;* University of Göttingen: Göttingen, Germany, 1997. (b) Sheldrick, G. M. *SHELXL-97, Program for the Refinement of Crystal Structures;* University of Göttingen: Göttingen, Germany, 1997.

(22) Sheldrick, G. M. In *Crystallographic Computing 3;* Sheldrick, G. M., Kruger, C., Goddard, R., Eds.; Oxford University Press: New York, 1985; pp 175−189.

(23) *teXsan: Crystal Structure Analysis Package;* Molecular Structure Corporation: The Woodlands, TX, 1985 and 2004.

Table 1. Donor−Acceptor Ratio, the First CT Absorption Band, Classification, and Conductivity Data of CT Complexes of **TTF-Im** Together with the Reduction Potential of Each Acceptor

	acceptor	E^A V[a]	D/A[c]	$h\nu_{CT}$[d] 10^3 cm^{-1}	class[e]	σ_{rt}[f] S cm^{-1} [E_a/meV]		acceptor	E^A V[a]	D/A[c]	$h\nu_{CT}$[d] 10^3 cm^{-1}	class[e]	σ_{rt}[f] S cm^{-1} [E_a/meV]
1	Me_2TCNQ	−0.23	1:1	6.4	N	8.9×10^{-5} [93]	**14**	DIDQ	+0.01	3:2	3.7	P	4.1×10^{-2} [93]
2	MeTCNQ	−0.19	1:1	3.2	P	3.3 [51]	**15**	QF_4	−0.37	2:1	3.1	P	2.7×10^{-1} [69]
3	TCNQ	−0.11	3:2	3.0	P	2.3 [50]	**16**	QCl_4	−0.39	2:1	2.7	P	120 [T_{MI}: ca. 180 K]
4	FTCNQ	−0.06	6:5	3.2	P	2.4×10^{-3} [99]	**17**	QBr_4	−0.39	2:1	3.0	P	4.3×10^{-1} [68]
5	F_2TCNQ	+0.02	3:2	3.2	P	4.0×10^{-5} [140]	**18**	QI_4	−0.48	2:1	6.3	N	3.8×10^{-4} [203]
6	CF_3TCNQ	+0.06	1:1	11.0	I	2.7×10^{-7} [339]	**19**	TNF	−0.82	1:1	12.3	N	$<10^{-9}$
7	F_4TCNQ	+0.19	2:1	3.8	P	5.4×10^{-1} [69]	**20**	TENF	−0.56	1:1	9.2	N	$<10^{-9}$
8	TCNE	−0.17	9:4	3.4	P	3.1×10^{-3} [94]	**21a**	I_2		1:1(I_5)	12.2	I	not measured[g]
9	DCNQ	−0.23	5:3	2.7	P	1.0×10^{-1} [72]	**21b**	I_2		3:2(I_3)	3.2	P	8.0×10^{-1} [95]
10	$Q(CN)_2$	−0.11	4:3	3.2	P	6.9×10^{-2} [77]	**22**	H_2CA	−0.69[b]	1:1	2.5	H/P	8.0×10^{-3} [92]
11	CBDQ	+0.08[b]	2:1	4.1	P	1.7×10^{-2} [97]	**23a**	H_2NA	−0.73[b]	5:4	3.2	H/P	9.2×10^{-3} [120]
12	DDQ	+0.09	2:1	4.3	P	1.5×10^{-1} [90]	**23b**	H_2NA	−0.73[b]	1:1	12.3	H/I	not measured[g]
13	DBDQ	+0.08	2:1	3.9	P	1.4×10^{-2} [99]	**24**	H_2CNAL	−0.75[b]	4:3	3.5	H/P	1.0×10^{-3} [133]

[a] First reduction potential of acceptors vs Fc/Fc^+ couple. [b] Peak potentials. [c] Molar ratios were estimated from the elemental analyses or determined by X-ray measurements. Some complexes contained crystal water or crystal solvent. [d] First CT absorption bands in KBr pellets. [e] Classification of the complexes. N: neutral; I: ionic; P: partial CT state of TTF moiety; and H: protonated state of the imidazole ring. In complexes **2** and **3**, acceptor moieties also possess partially ionic states. [f] Electrical conductivity was measured by the four- or two-probe method on a compressed pellet except for that of **16**. [g] Conductivity was not measured for **21a** and **23b** because of the small amount of samples and the contamination by the other phase complexes.

which indicates the formation of strong intermolecular H-bond interaction between donor molecules, between donor and acceptor molecules, or between donor and solvent molecules. Table 1 summarizes the properties of CT complexes: the first reduction potentials of acceptors (E^A), donor−acceptor ratios, the first CT absorption bands in KBr pellet ($h\nu_{CT}$), classification of complexes (N/P/I/H; see Table 1), and electrical conductivities at room temperature (σ_{rt}) together with activation energies (E_a). The E^A values of anilic acids (H_2CA, H_2NA, and H_2CNAL) were determined in the neutral state. The CV measurements of mono- and dianion salts of H_2CNAL show no reduction peaks, and thus their neutral species seem to oxidize **TTF-Im** during the complex formation.

Neutral CT Complexes. The 1:1 complexes (**1**, **19**, and **20**) and 2:1 QI_4 complex (**18**) are characterized as neutral ones (class N). The characterization was performed by the comparison of their IR spectra to those of the neutral acceptors and their radical anions (C≡N stretching mode at 2204 cm^{-1} for **1**[24] and the C═O stretching mode at 1656 cm^{-1} for **18**[25]). The radical anion salts of TNF and TENF are unknown; however, the IR spectra of **19** and **20**, which are almost simple superimpositions of **TTF-Im** and each acceptor, indicate that they are neutral complexes. These observations agree with intermolecular bond length analysis in the crystal structures of **1** and **20** (Tables S4 and S6 in Supporting Information). The CT bands ($6.3-12.3 \times 10^3$ cm^{-1}) of these complexes are assigned as intermolecular CT transitions from donor to acceptor in a neutral ground state. These complexes exhibited low electrical conductivity (compressed pellets, $\sigma_{rt} = 8.9 \times 10^{-5}$ S cm^{-1} for **1**, $\sigma_{rt} = 3.8 \times 10^{-4}$ S cm^{-1} for **18**, and $\sigma_{rt} < 10^{-9}$ S cm^{-1} for **19** and **20**). In the measurement of variable-temperature IR spectra of **1** and **18**, any distinct behaviors indicating neutral ionic transition were not found (Figures S12 and S14 in Supporting Information).

Figure 1 shows the crystal structure of Me_2TCNQ complex **1**, where crystallographically independent **TTF-Im**, two kinds of Me_2TCNQ (Me_2TCNQ-A and -B on special positions), and MeCN solvent molecules are included. **TTF-Im** and MeCN molecules formed a H-bond with the N−H···N≡C distance of 3.012(4) Å (Figure 1a). Donor and acceptor molecules formed a DADA alternating stack column along the [0$\bar{1}$1] direction with face-to-face distances of ca. 3.6 Å for **TTF-Im**−Me_2-TCNQ-A and ca. 3.4 Å for **TTF-Im**−Me_2TCNQ-B (Figure 1b). **TTF-Im** molecules formed a dimer by side-by-side S···S interactions (S1···S3, 3.454(1) Å), which connected the DADA columns (Figure 1b).

The crystal structure of **20** is illustrated in Figure 2. Two **TTF-Im** (A and B), two TENF (A and B), and one MeCN molecules were crystallographically independent. Neighboring **TTF-Im**-B, **TTF-Im**-A, and MeCN molecules were linked via H-bonds, forming a D−D−MeCN pair (Figure 2a). The H-bond distances between **TTF-Im**-B···**TTF-Im**-A and between **TTF-Im-A···MeCN** were 2.964(3) and 2.940(3) Å, respectively. Each **TTF-Im**-A and -B formed alternating columns with TENF-A and -B, respectively (Figure 2b). The face-to-face distances were

(24) The C≡N stretching frequencies of Me_2TCNQ; neutral: 2222, 2210 cm^{-1} and $Me_2TCNQ^{\bullet-}$: 2183, 2164 cm^{-1}.
(25) The C═O stretching frequencies of QI_4; neutral: 1662 cm^{-1} and $QI_4^{\bullet-}$: 1498 cm^{-1}. See: Matsuzaki, S.; Hiejima, T.; Sano, M. *Bull. Chem. Soc. Jpn.* **1991**, *64*, 2052−2057.

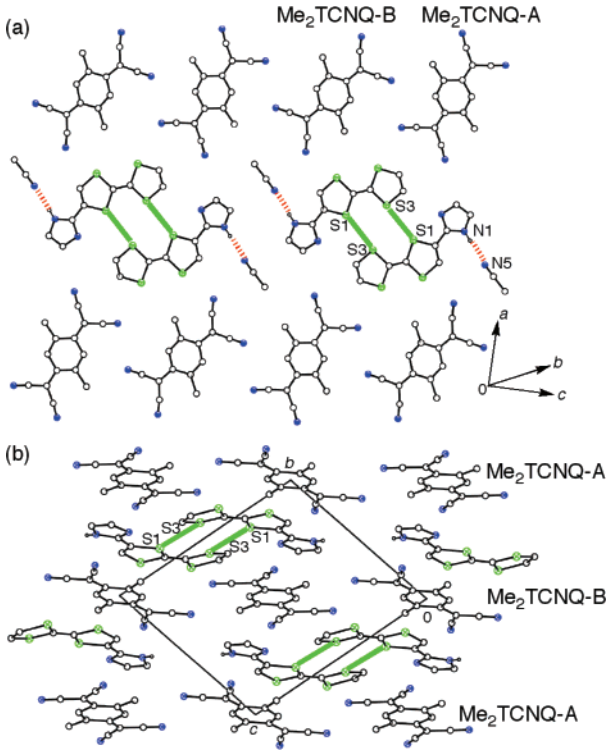

Figure 1. Crystal structure of the Me_2TCNQ complex **1**. (a) Arrangement of donor and acceptor molecules viewed along the nearly perpendicular direction to molecular plane showing the H-bond between donor and MeCN (red dotted lines) and S···S interactions (green lines). (b) Perspective view along the *a*-axis showing the alternating columnar structure and intercolumn S···S interactions.

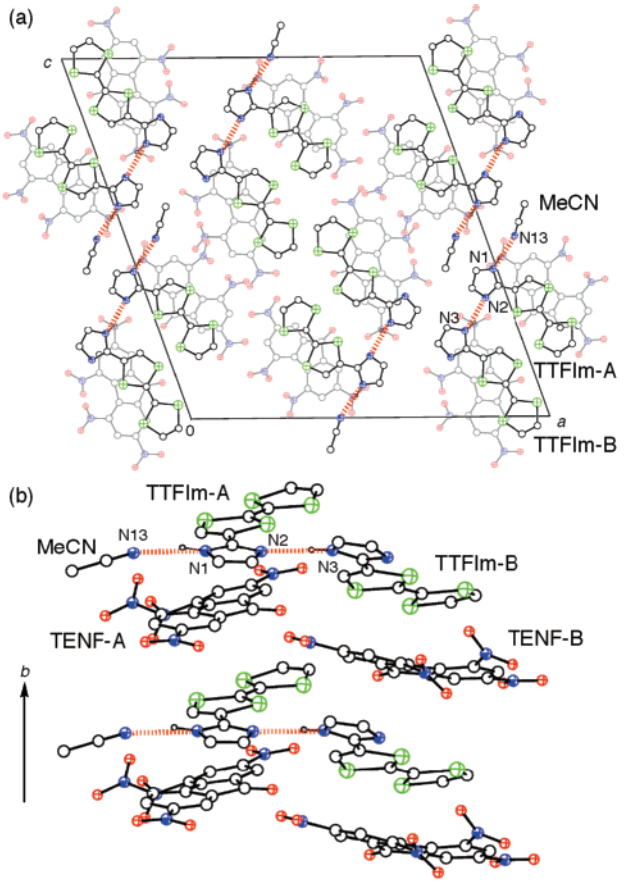

Figure 2. Crystal structure of the TENF complex **20**. (a) Perspective view along the *b*-axis showing D−D−MeCN H-bonded pair and molecular packing. Gray molecules are TENF. (b) DADA columns and D−D−MeCN pair. Red dotted lines show N−H···N H-bonds.

ca. 3.3−3.4 Å for the **TTF-Im**-A−TENF-A column and ca. 3.5−3.8 Å for the **TTF-Im**-B−TENF-B column.

Ionic CT Complexes. The complexes in this class (I), **6** and **21a**, showed intermolecular CT absorptions induced between neighboring **TTF-Im**$^{\bullet+}$ species at 11.0 and 12.2 × 10^3 cm^{-1}, respectively, in the electronic spectra, and a low-energy CT band at around 5.0 × 10^3 cm^{-1} was not found.

In the crystal structure analysis of **21a**, (**TTF-Im**$^{\bullet+}$)(I_5^-), each of two crystallographically independent donor molecules (**TTF-Im**-A and -B) formed face-to-face dimers with the same kind of **TTF-Im** (Figure 3a), being in accord with the observation of intradimer CT transition in the electronic spectra. The dimers possessed a head-to-tail fashion, and the face-to-face distances were 3.47 Å for **TTF-Im**-A−A and 3.41 Å for **TTF-Im**-B−B. Imidazole rings of **TTF-Im**-A and -B were alternately connected by N−H···N H-bonds and formed a one-dimensional zigzag chain along the *a*-axis (Figure 3a). The H-bond distances were 2.86(2) Å for N1−H···N4 and 2.90(2) Å for N3−H···N2. Neighboring imidazole rings connected by H-bonds were nearly perpendicular (88.67°) to each other. These face-to-face dimerizations of TTF moiety and H-bond interactions of imidazole rings formed a two-dimensional stairlike structure (Figure 3a). Iodine atoms in **21a** formed a I_{10}^{2-} cyclic structure and a $(I_5^-)_x$ zigzag infinite chain structure (Figure 3b−d).[26] The I···I bond lengths in these units are consistent with those of known structures and indicate that the I_{10}^{2-} unit is composed of two I_3^- units (I1−I3) and two I_2 units (I4 and I5) and that the $(I_5^-)_x$ chain is composed of I_3^- (I6−I8) and I_2 (I9 and I10) units (Table S7 in Supporting Information).

Partial CT Complexes. Complexes **2**−**5** and **7**−**17** belonged to this class (P). In the 3:2 TCNQ complex **3**, C═C stretching modes of TCNQ moiety at 1416 and 1430 cm^{-1} in the Raman spectrum indicated the charge separation of TCNQ moiety with the ionicities of −0.4 and −0.6 (Figure S4 in Supporting Information).[27] The appearance of two C≡N stretching modes at 2215 and 2198 cm^{-1} in the IR spectrum (Figure S5 in Supporting Information) also implied the charge separation of TCNQ moiety.[28] As for the **TTF-Im** moiety, one C═C stretching mode in the Raman spectrum was observed at 1448 cm^{-1}, which exists between neutral **TTF-Im** (1521 cm^{-1}) and (**TTF-Im**$^{\bullet+}$)(I_5^-) (**21a**, 1413 cm^{-1}). These measurements indicate that both **TTF-Im** and TCNQ molecules in **3** are in the partial CT states. The low-energy CT absorption in the electronic spectra of 1:1 MeTCNQ complex **2** indicates the partial CT state. The appearance of two C≡N stretching modes (2210 and

(26) (a) Svensson, P. H.; Kloo, L. *Chem. Rev.* **2003**, *103*, 1649−1684. (b) Wieczorrek, C. *Acta Crystallogr., Sect. C* **2000**, *56*, 1082−1084.

(27) Matsuzaki, S.; Kuwata, R.; Toyoda, K. *Solid State Commun.* **1980**, *33*, 403−405.

(28) Chappell, J. S.; Bloch, A. N.; Bryden, W. A.; Maxfield, M.; Poehler, T. O.; Cowan, D. O. *J. Am. Chem. Soc.* **1981**, *103*, 2442−2443. The C≡N stretching frequency of TCNQ derivatives is known to exhibit lower-frequency shift with the increase of ionicity and has been utilized as a simple tool to estimate the ionicity and electronic structure of CT complex. However, the C≡N stretching frequency is sensitive also to the environmental perturbations such as H-bond, and the estimation of ionicity often gives an inaccurate value. Furthermore, the appearance of a symmetric mode causes the inaccurate estimation for the ionicity to be more negative than ca. −0.5.

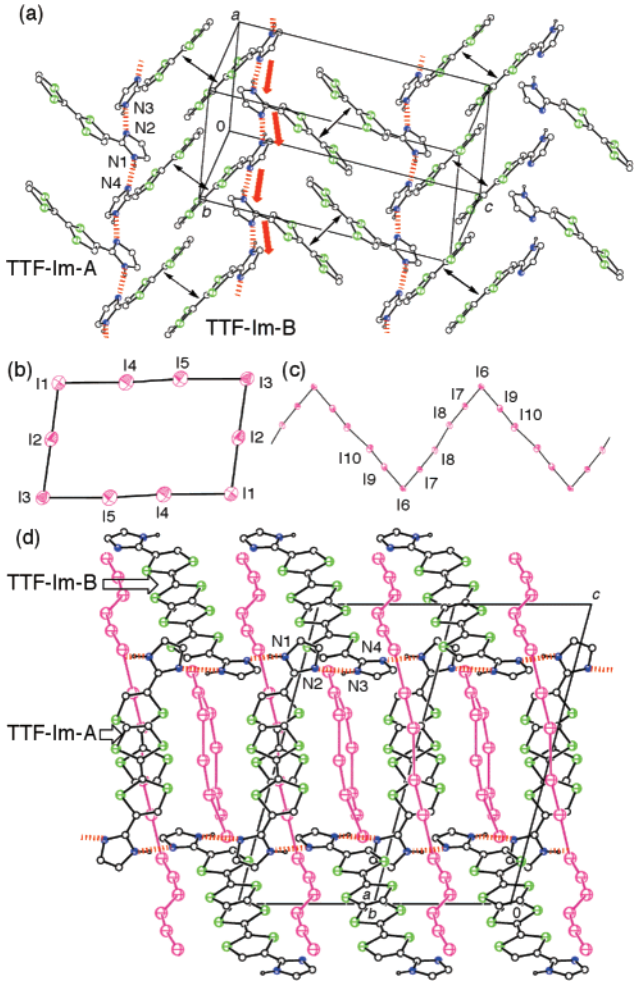

Figure 3. Crystal structure of the I_5^- complex **21a**. (a) Two-dimensional structure by N−H···N H-bonds of imidazole ring (red dotted lines) and dimerization of TTF skeletons (double head arrows). Anion moieties were omitted. (b and c) Structures of the I_{10}^{2-} ring and $(I_5^-)_x$ chain, respectively. (d) Crystal packing viewed along the [1$\bar{1}$0] direction. Purple molecules indicate I_{10}^{2-} ring and $(I_5^-)_x$ chain.

2188 cm^{-1}; Figure S5 in Supporting Information)[28,29] similar to that in **3** implies the charge separation of the acceptor moiety.

For the complexes **4**, **5**, and **7**−**17**, acceptor moieties are characterized as fully ionic radical anions from the resemblances in C≡N, C═O, and C═C stretching modes in the IR spectra to those of radical anion salts of each acceptor. Because these complexes possess excess donor molecules, **TTF-Im** moieties are in the partial CT state (averaged charges on **TTF-Im** moiety: +0.44 to +0.83). Complexes in this class exhibited low-energy CT absorption bands at 2.7−4.3 × 10^3 cm^{-1}, confirming the partial CT state (Figure 4). This band is assigned as an intracolumnar CT transition of partial CT complex having a segregated structure and is a necessary condition for a highly conductive complex.[30] The conductivity measurements (compressed pellets except for **16**) showed high values of $\sigma_{rt} = 10^{-3}$ to 10^2 S cm^{-1} except for the complex **5** ($\sigma_{rt} = 4.0 \times 10^{-5}$ S cm^{-1}). Especially the QCl_4 complex **16** exhibited a metallic behavior down to 180 K with high σ_{rt} value of 120 S cm^{-1}

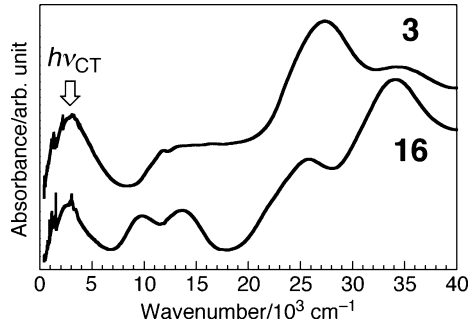

Figure 4. Electronic spectra of complexes **3** and **16** in KBr pellets.

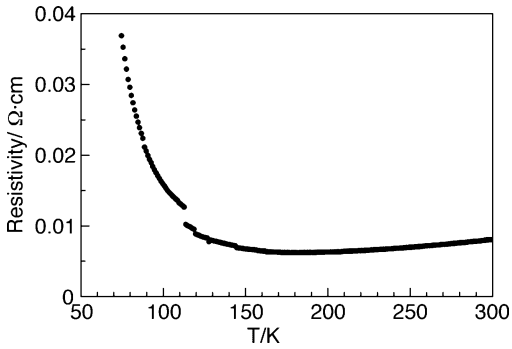

Figure 5. Temperature dependence of the resistivity of complex **16** measured along the stacking direction (*a*-axis).

(Figure 5). Below 180 K, the resistivity gradually increased without any abrupt phase transition, which is supported by the magnetic measurements[20] and variable-temperature IR spectra (Figure S13 in Supporting Information). This complex is the first example of the purely organic metallic CT complex composed of H-bond functionalized TTF derivatives.

In the crystal structure, complex **16** is composed of two **TTF-Im** molecules and one QCl_4 molecule having an inversion center (Figure 6). The intramolecular bond lengths of QCl_4 moiety are close to those of $QCl_4^{\bullet-}$ salt[31] (Table S5 in Supporting Information). From these observations, the ionicity of QCl_4 moiety is estimated as −1, and thus that of **TTF-Im** is +0.5, a partial CT state. Complex **16** formed a D−A−D triad by N(1)−H···O(1)═C H-bond with the distance of 2.800(4) Å (Figure 6a) by site-selective molecular recognition of imidazole moieties to oxygen atoms of QCl_4 molecule. The accumulation of this D−A−D unit constructed the 2:1 D−A ratio of this complex. Both donor and acceptor molecules stacked uniformly along the *a*-axis and formed a segregated structure (Figure 6). The face-to-face distances in stacking columns of **TTF-Im** and QCl_4 were 3.46 and 3.19 Å, respectively. The side-by-side S···S contacts on TTF skeleton (3.568(1) Å for S(1)···S(4) and 3.513-(1) Å for S(2)···S(3)) connected the **TTF-Im** columns and formed a two-dimensional donor layer (Figure 6b). The intermolecular overlap integrals along the side-by-side direction and calculated Fermi surface indicate a quasi-one-dimensional feature.[20]

PT-Coupled CT Complexes. The anilic acid-type acceptors (H_2CA, H_2CNAL, and H_2NA) show two-step PT processes (Chart 1). Thus, the complex formation of **TTF-Im** with anilic acids is expected to cause both CT on the TTF moiety and PT

(29) The C≡N stretching frequency of MeTCNQ; neutral: 2223 cm^{-1} and $MeTCNQ^{\bullet-}$: 2189, 2172 cm^{-1}.
(30) (a) Torrance, J. B.; Scott, B. A.; Kaufman, F. B. *Solid State Commun.* **1975**, *17*, 1369−1373. (b) Torrance, J. B.; Scott, B. A.; Welber, B.; Kaufman, F. B.; Seiden, P. E. *Phys. Rev. B* **1979**, *19*, 730−741.
(31) (a) Weperen, K. J.; Visser, G. J. *Acta Crystallogr., Sect. B* **1972**, *28*, 338−342. (b) Zanotti, G.; Del Pra, A. *Acta Crystallogr., Sect. B* **1980**, *36*, 313−316.

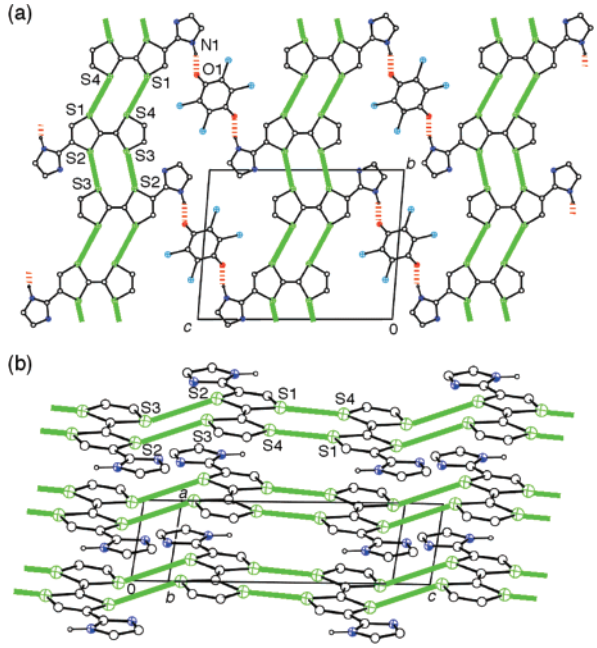

Figure 6. Crystal structure of the QCl_4 complex **16**. (a) Perspective view along the *a*-axis showing the D−A−D triad by N−H···C═O H-bonds (red dotted lines) and the side-by-side S···S interactions on TTF skeleton (green lines). (b) Packing pattern of the **TTF-Im** molecules in the conduction layer.

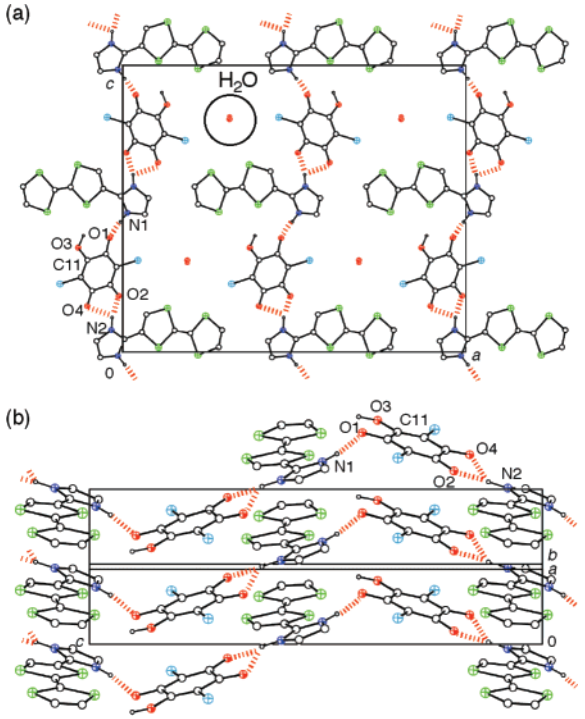

Figure 7. Crystal structure of the H_2CA complex **22**. (a) Perspective view along the *b*-axis showing the one-dimensional H-bonded structure. (b) Two-dimensional layer structure by H-bonds and the uniform π-stacking. H-bonds are indicated by red dotted lines.

on the imidazole ring[32] as shown in Scheme 1. Several CT complexes of anilic acids with TTF derivatives have been prepared;[33] however, no radical anion species of anilic acids but only deprotonated closed-shell anion species have been obtained.

PT Complex. The 1:1 H_2CA complex **22** was characterized as a PT complex (class H) from the IR spectra and X-ray analysis. In this complex, H_2CA acted as a proton donor rather than an electron acceptor. The acceptor moiety in **22** was assigned as a monodeprotonated HCA^- from the C═O stretching frequencies in the IR spectrum at 1677, 1620, and 1550 cm^{-1}, which resemble those of HCA^- salt (1680, 1637, and 1538 cm^{-1}).[33d] The C−O bond lengths of the HCA^- moiety also indicate the monodeprotonated form and shows that the residual proton is located at the O3 atom (Figure S10 in Supporting Information).[32a,33d] The C−N−C angles around both N1 and N2 atoms (109.5(7)° and 107.2(8)°, respectively) are larger than those of unprotonated nitrogen atoms in **1**, **16**, **20**, and **21a** (104−105°) (Table S3 in Supporting Information) and showed that both N1 and N2 atoms are protonated. The central C−C bond length in TTF skeleton (1.33(1) Å) is close to that of neutral **TTF-Im** (1.339(4) Å) (Table S2 in Supporting Information). These observations indicate the protonated form of

donor molecule **TTF-Im·H**$^+$. In the crystal structure of **22**, N−H···O H-bonds between the imidazole ring and HCA^- formed a one-dimensional chain along the *c*-axis (Figure 7a). The H-bond distances were 2.768(9) Å for N(1)−H···O(1), 2.68(1) Å for N(2)−H···O(2), and 3.124(9) Å for N(2)−H···O(4). This H-bonded structure is very similar to that shown in the HCA^- salt of imidazolium.[32a] Both components formed uniform one-dimensional columns along the *b*-axis with the face-to-face distances of 3.43 Å for **TTF-Im·H**$^+$ and 3.26 Å for HCA^- (Figure 7b). There was no short S···S contact between TTF skeletons. The H_2O molecule was included in the channel structure parallel to the column structure (ca. 5 Å of diameter) and disordered (Figure 7a).

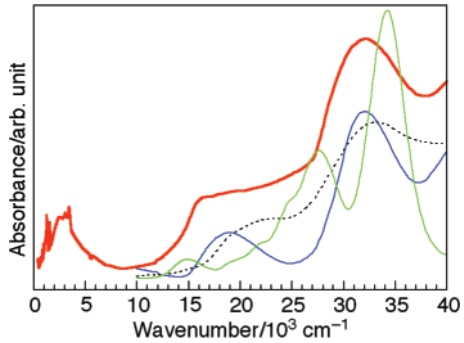

Figure 8. Electronic spectra of complex **22** (red line) in KBr pellet together with (**TTF-Im·H**$^+$)(Br^-) (dotted line), (Bu_4N^+)(HCA^-) salt[34] (blue line), and **21a** in MeCN (green line).

Despite the assignment of **22** as a simple PT complex, the measurement of electrical conductivity showed a high value for the PT complex, $\sigma_{rt} = 8.0 \times 10^{-3}$ S cm^{-1}. The electronic spectra showed a low energy absorption band (~3000 cm^{-1}) assignable as an intermolecular CT transition from neutral TTF moiety to radical cation species (Figure 8).[30] The broad tail at around 10−15 $\times$ 10^3 cm^{-1}, which was not observed in HCA^- (>15 $\times$ 10^3 cm^{-1}) and **TTF-Im·H**$^+$ (>16 $\times$ 10^3 cm^{-1}) salts, indicates the

(32) (a) Ishida, H.; Kashino, S. *Acta Crystallogr., Sect. C* **2001**, *57*, 476−479. (b) Wang, Z.-L.; Wei, L.-H. *Acta Crystallogr., Sect. E* **2005**, *61*, o3129−o3130.

(33) (a) Zaman, Md. B.; Toyoda, J.; Morita, Y.; Nakamura, S.; Yamochi, H.; Saito, G.; Nakasuji, K. *Synth. Met.* **1999**, *102*, 1691−1692. (b) Zaman, Md. B.; Toyoda, J.; Morita, Y.; Nakamura, S.; Yamochi, H.; Saito, G.; Nishimura, K.; Yoneyama, N.; Enoki, T.; Nakasuji, K. *J. Mater. Chem.* **2001**, *11*, 2211−2215. (c) Morita, Y.; Maki, S.; Ohmoto, M.; Kitagawa, H.; Okubo, T.; Mitani, T.; Nakasuji, K. *Org. Lett.* **2002**, *4*, 2185−2188. (d) Kabir, Md. K.; Tobita, H.; Matsuo, H.; Nagayoshi, K.; Yamada, K.; Adachi, K.; Sugiyama, Y.; Kitagawa, S.; Kawata, S. *Cryst. Growth Des.* **2003**, *3*, 791−798.

existence of **TTF-Im**$^{\bullet+}$ (>12 × 10^3 cm^{-1}) or **TTF-Im**$^{\bullet+}$·**H**$^+$ species. In the Raman spectra, **22** exhibited a C═C stretching mode (1472 cm^{-1}) assignable as that of partially oxidized **TTF-Im** or **TTF-Im·H**$^+$ species (Figure S4 in Supporting Information). This observation confirms that **22**, which is essentially a PT complex, contains a small amount of radical cation species of TTF moiety as impurity. Probably, the proton of a part of HCA^- moiety would dissociate during the complex formation, resulting in the formation of CA^{2-} and **TTF-Im**$^{\bullet+}$·**H**$^+$.[35] Accordingly, composition of **22** could be represented as (**TTF-Im·H**$^+$)$_{1-x}$(**TTF-Im**$^{\bullet+}$·**H**$^+$)$_x$(HCA^{-1})$_{1-x}$(CA^{2-})$_x$(H_2O)$_{0.7}$ ($0 < x < 1$).

Partial CT and PT Complexes. The donor molecules in the complexes **23a** and **24** were composed of partially ionized TTF skeleton and protonated imidazole ring (class H/P). The acceptor moiety in **24** is assigned as a dianion, $CNAL^{2-}$, from the resemblance in C═O stretching frequency in the IR spectrum (1546 cm^{-1} for **24**, 1559 cm^{-1} for neutral H_2CNAL, 1575 cm^{-1} for (Bu_4N^+)($HCNAL^-$), and 1555 cm^{-1} for (Bu_4N^+)$_2$($CNAL^{2-}$)).[36] As for complex **23a**, the similarity of C═O stretching modes to those of **23b** in the IR spectra indicates the dianionic state of acceptor, NA^{2-}. Considering a balance of charge and an existence of the low-energy CT band, the donor molecules in these complexes seem to have a protonated imidazole ring and a partially ionized TTF moiety. Since **23a** and **24** have 5:4 and 4:3 D−A ratios, respectively, their donor molecules are presented as **TTF-Im**$^{x\bullet+}$·*y***H**$^+$, where $5(x + y) = 8$, $0.6 \le x,y \le 1$, and $4(x + y) = 6$, $0.5 \le x,y \le 1$, respectively. These complexes were also relatively conductive semiconductors with σ_{rt} values of 9.2 × 10^{-3} S^{-1} cm^{-1} for **23a** and 1.0 × 10^{-3} S cm^{-1} for **24**.

Completely CT and PT Complex. The donor molecule in **23b** was characterized as a radical dication, **TTF-Im**$^{\bullet+}$·**H**$^+$ (class H/I). In the crystal structure analysis, this complex was composed of a 1:1:1 ratio of donor, acceptor, and MeCN solvent. The short C−O bond lengths of acceptor moiety (1.23−1.25 Å) indicate the dideprotonated form, NA^{2-} (Figure S11 in Supporting Information).[37] The central C−C bond length of TTF skeleton (1.393(4) Å) and C−N−C angles in imidazole ring (108.2(3)° and 108.7(3)° for N1 and N2, respectively) show the radical dication state, **TTF-Im**$^{\bullet+}$·**H**$^+$ (Tables S2 and S3 in Supporting Information). H-bonds between **TTF-Im**$^{\bullet+}$·**H**$^+$ and NA^{2-} formed a cyclic motif composed of two donors and two acceptors (Figure 9a). N···O distances within a cyclic motif were N1···O1, 2.643(4); N1···O2, 3.024(4); N2···O2, 2.755(3); and N2···O5, 2.758(4) Å. The face-to-face dimerization on TTF skeletons (3.36 Å) and NA^{2-} molecules (3.30 Å) linked the cyclic motifs, forming a two-dimensional structure (Figure 9b). In the electronic spectra, this complex showed an absorption at 12.3 × 10^3 cm^{-1} assignable as a CT band within the **TTF-Im**$^{\bullet+}$·**H**$^+$ dimer, which is consistent with the crystal structure.

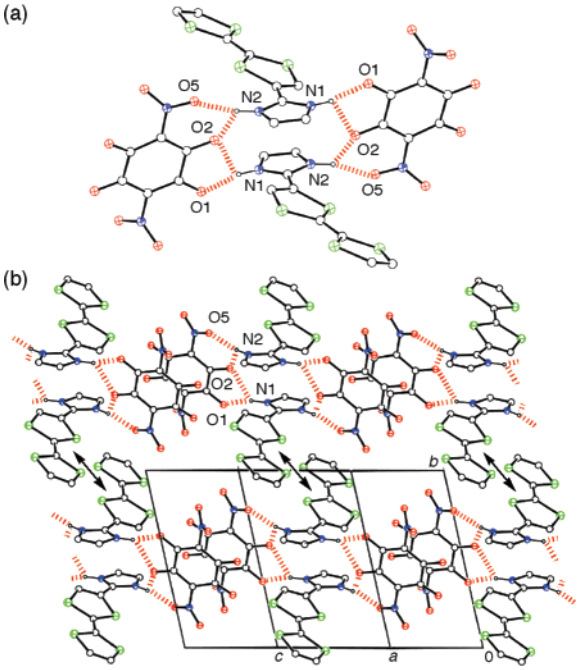

Figure 9. Crystal structure of the H_2NA complex **23b**. (a) H-bonded cyclic unit composed of two donors and two acceptors. (b) Two-dimensional structure by H-bonds and face-to-face dimerization. Red dotted lines indicate H-bonds, and double head arrows shows face-to-face dimerizations.

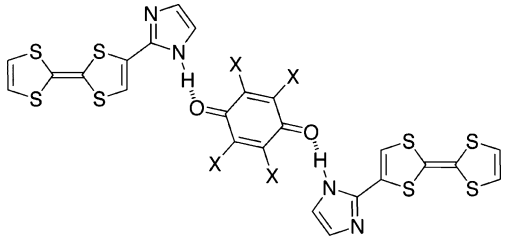

Figure 10. Schematic view of the D−A−D H-bonded triad composed of two **TTF-Im** molecules and *p*-benzoquinone-type acceptors.

Roles of H-Bonds in CT Complexes. One of the features of **TTF-Im** CT complexes is that many of them have no 1:1 D−A ratio and are a donor-excess system (Table 1). Especially complexes with the *p*-benzoquinone-type electron acceptors, **11**−**13** and **15**−**18**, have 2:1 D−A ratio. As shown in the QCl_4 complex **16**, these complexes are expected to be composed of the D−A−D triad, which is formed by H-bonds between the imidazole ring and carbonyl group in the acceptors (Figures 6a and 10). This result shows a keen difference from those of pristine TTF−*p*-benzoquinone systems, most of which possess 1:1 D−A ratios with low electrical conductivities ($\sigma_{rt} < 10^{-4}$ S cm^{-1}), excepting DCNQ (3:2, $\sigma_{rt} = 1$ S cm^{-1}),[38] QF_4 (1:1 neutral complex, but $\sigma_{rt} = 10$ S cm^{-1}),[39] QBr_4 (2:1 neutral complex, insulator),[40] and QI_4 (2:1 neutral complex, insulator).[25] The donor-excess composition in other partial CT complexes strongly implies the formation of a D−A−D H-bonded triad or similar structure.

The other feature of the present system is that donor-excess complexes including those of weak acceptors **15**−**17** have

(34) Preparation of (Bu_4N^+)(HCA^-) will be reported elsewhere.
(35) In the thermal factor of H atoms in the X-ray analysis, any evidence of the deprotonation of HCA^- was not found because of the very small amount of CA^{2-} species. A similar proton defect causing the conflict between formal charge and real charge has been observed in a TCNQ complex of palladium−ethylenediaminoglyoxymate. See: Itoh, T.; Toyoda, J.; Tadokoro, M.; Kitagawa, H.; Mitani, T.; Nakasuji, K. *Chem. Lett.* **1995**, *24*, 41−42.
(36) Preparation of (Bu_4N^+)($HCNAL^-$) and (Bu_4N^+)$_2$($CNAL^{2-}$) will be reported elsewhere.
(37) Andersen, E. K.; Andersen, I. G. K. *Acta Crystallogr., Sect. B* **1975**, *31*, 379−383.
(38) Bryce, M. R.; Davies, S. R.; Hasan, M.; Ashwell, G. J.; Szablewski, M.; Drew, M. G. B.; Short, R.; Hursthouse, M. B. *J. Chem. Soc., Perkin Trans. 2* **1989**, 1285−1292.
(39) Torrance, J. B.; Mayerle, J. J.; Lee, V. Y.; Bechgaard, K. *J. Am. Chem. Soc.* **1979**, *101*, 4747−4748.
(40) Sadohara, R.; Matsuzaki, S. *Mol. Cryst. Liq. Cryst.* **1997**, *296*, 269−280.

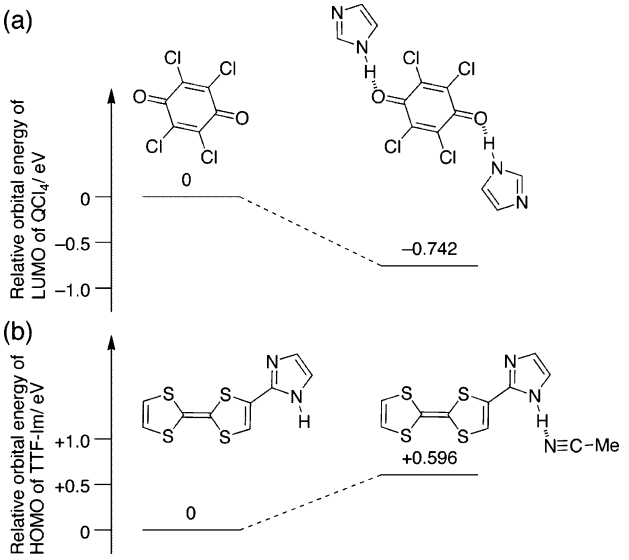

Figure 11. (a) Comparison of calculated LUMO energies of QCl_4 without H-bonds with imidazole ring (left) and in the imidazole−QCl_4−imidazole triad which was shown in complex **16** (right). (b) Comparison of calculated HOMO energies of isolated **TTF-Im** (left) and of that forming H-bond with MeCN molecule as shown in complex **1** (right). The structures were extracted from crystal structures of **16** and **1**, respectively.

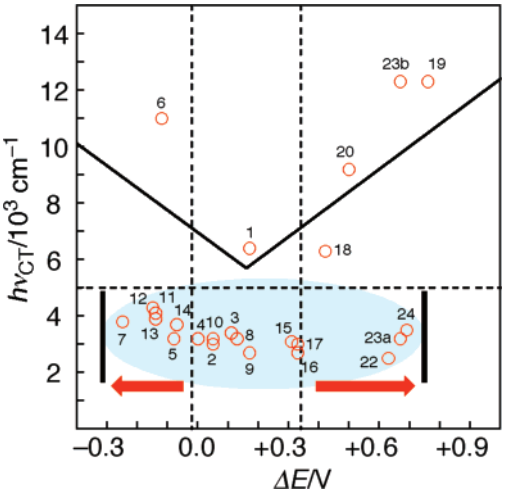

Figure 12. Plot of the first CT absorption bands in solid ($h\nu_{CT}$) against the difference of the first redox potentials between **TTF-Im** and acceptors (ΔE), where the highly conductive region was greatly expanded by electronic modulation of H-bond (blue ellipse circle).[4a] Numbers indicate those of CT complexes in Table 1. The V-shaped line, and vertical and horizontal dotted lines are explained in the text.

completely ionic acceptor moieties (Table 1). The pristine TTF−tetrahalo-*p*-benzoquinone systems exist at the boundary of neutral and ionic systems and give several polymorphs (neutral, partial CT, and ionic complexes) depending on the preparation conditions.[25,39−41] In contrast, the complex formation of **TTF-Im**, which has an electron-donating ability similar to that of pristine TTF, with QCl_4 under various conditions (direct mixing, diffusion, and co-sublimation methods under 1:2−2:1 molar ratios) gave only one kind of CT complex **16**. Namely, **TTF-Im** suppresses complex isomerism and readily gives completely ionic acceptor moiety in the complex formation even with relatively weak acceptors. This origin can be explained by the polarizability of H-bonds, where H-bond induces the negative and positive charges at the proton-donor and -acceptor atoms, respectively. To confirm this hypothesis, we examined the DFT calculation on an imidazole−QCl_4−imidazole H-bonded unit, where the atomic orientations were extracted from the crystal structure of complex **16**.[42] Actually, the calculated atomic charge suggests that the N−H···O═C H-bond induces more negative and positive charges on the carbonyl carbon and oxygen atoms in QCl_4, respectively (+0.48 and −0.42 in isolated QCl_4, and +0.50 and −0.45 in QCl_4 of the triad, respectively; Table S9 in Supporting Information). Furthermore, the calculation showed a distinguishable lowering of the LUMO level of the QCl_4 moiety (Figure 11a). This result indicates that the formation of the H-bond with imidazole ring increases an electron-accepting ability of the QCl_4 moiety, causing the complete ionization of the acceptor moiety in the complex **16**. In the same calculation on the **TTF-Im**−QCl_4−**TTF-Im** triad in **16**, the electrostatic potential indicates that more negative charge is attracted on oxygen atoms of QCl_4 by the formation of the H-bond (Figure S15 in Supporting Information). Furthermore, sums of atomic charges for **TTF-Im** and QCl_4 moieties are calculated as +0.4 and −0.8 (Table S10 in Supporting Information), respectively, suggesting the CT between **TTF-Im** and QCl_4. Such electronic effect of the H-bond has been experimentally pointed out by the electrochemical measurement of *p*-benzoquinone-type electron acceptors under the existence of alcohol as the H-bond source in a solution state.[43,44]

In addition, H-bond formation enhances the electron-donating ability of **TTF-Im**. In the (DADBTTF)(TCNQ)(MeCN) complex, the theoretical calculation shows that the H-bonds of amino group with MeCN increase the HOMO level of DADBTTF by ca. 0.33 eV.[10] In the amido-substituted TTF system, H-bond formation with guest molecules or anion enhances the electron-donating ability by 0.03−0.11 V, as experimentally demonstrated in electrochemical measurement.[8b,11]

The calculation on the Me_2TCNQ complex **1**, where **TTF-Im** forms the H-bond with MeCN molecule, pointed out that the HOMO level of **TTF-Im**−MeCN H-bonded diad is higher than that of the isolated **TTF-Im** (Figure 11b). Despite this effect, complex **1** was a neutral complex. The reasons for this result seem to be the absence of H-bonds between donor and acceptor molecules as shown in its crystal structure (Figure 1). In the QI_4 complex **18**, the very weak electron-accepting ability of QI_4 ($E^A = -0.48$ V) resulted in the neutral ground state.

The 2:1 D−A ratio and the acceptor ionicity of −1 in the complexes with *p*-benzoquinone-type acceptors **11**−**13** and **15**−**17** controlled the ionicity of donor molecules to be +0.5 and the partial CT state. Figure 12 shows the plot of $h\nu_{CT}$ vs differences between E^D and E^A (ΔE).[45] The V-shaped line (bold face line) in the plot shows the theoretical CT transition energies

(41) (a) Torrance, J. B.; Girlando, A.; Mayerle, J. J.; Crowley, J. I.; Lee, V. Y.; Batail, P.; LaPlaca, S. J. *Phys. Rev. Lett.* **1981**, *47*, 1747−1750. (b) Mayerle, J. J.; Torrance, J. B.; Crowley, J. I. *Acta Crystallogr., Sect. B* **1979**, *35*, 2988−2995. (c) Girlando, A.; Pecile, C.; Torrance, J. B. *Solid State Commun.* **1985**, *54*, 753−759.

(42) To exclude the effect of CT between **TTF-Im** and QCl_4, TTF skeleton was removed in the calculation. The H atom at the 2-position of the imidazole ring was placed in accordance with the configuration of the C atom in the imidazole ring and the C−H bond length of 1.0 Å.

(43) We have examined the CV measurement for mixture of **TTF-Im** and QCl_4 in a MeCN solution. However, probably because of the H-bond formation with solvent and/or supporting electrolyte, redox potentials of both molecules did not change significantly. See Figure S9 in the Supporting Information.

(44) (a) Gupta, N.; Linschitz, H. *J. Am. Chem. Soc.* **1997**, *119*, 6384−6391. (b) Uno, B.; Okumura, N.; Goto, M.; Kano, K. *J. Org. Chem.* **2000**, *65*, 1448−1455.

of the D−A pairs in neutral (right) and ionic (left) complexes.[4a] Generally, highly conductive complexes have a partial CT ground state and a segregated stack structure and exhibit a low-energy intermolecular CT band.[30] Their plots deviate from the V-shaped line and appear at a $h\nu_{CT}$ region lower than ca. 5×10^3 cm^{-1} (horizontal dotted line). In well-known low-dimensional TTF systems, CT complexes showing low-energy absorption bands are obtained only in the ΔE region of $-0.02 < \Delta E < +0.34$ V (vertical dotted lines) for the TTF−TCNQ system and $-0.04 < \Delta E < +0.31$ V for the TTF−*p*-benzoquinone system which are proposed as the regions of "a high probability of being organic metals".[1d,4] In the **TTF-Im** system, this region is widely expanded to $-0.25 < \Delta E < +0.69$ V, and especially all *p*-benzoquinone-type acceptors gave the low-energy CT complexes except for **18**. This result is surprisingly different from the pristine TTF system and clearly reveals that the electronic modulation by H-bonds to control ionicity of each component is remarkably effective in the development of conductive CT complexes.

The robust and directional H-bonds of **TTF-Im** are useful also in the structural regulation.[7] The direct N−H···N H-bonds of imidazole rings formed a one-dimensional zigzag chain in I_5 salt **21a** (Figure 3a), which has been observed also in several imidazole derivatives[16] and neutral **TTF-Im**.[20] The one-dimensional D−A−D−A H-bonded structure in the H_2CA complex **22** (Figure 7a) was very similar to that shown in the imidazolium−HCA^- salt.[32a] These results confirm that the robust and directional natures of H-bond interactions are prior in the construction of molecular packing. In the QCl_4 complex **16**, the N−H···O═C H-bonds between donor and acceptor connected the donor layers across the acceptor molecule (Figure 6a). This H-bond increased the dimensionality of the network structure, resulting in the prevention of the abrupt insulating transition such as Peierls-type transition.[4]

(45) The E^D value would be affected (reduced) by the H-bond of **TTF-Im** with solvent (DMF) or supporting electrolyte (ClO_4^-), however, we could not remove the effect. From the CV measurements under different conditions (solvent: CH_2Cl_2, MeCN, and THF; supporting electrolyte: $Bu_4N^+ClO_4^-$ and $Bu_4N^+PF_6^-$), the ΔE region for conducting CT complexes was determined as -0.25 to $-0.16 < \Delta E < +0.69$ to $+0.96$.

Summary

The donor−acceptor CT complex formation of a new TTF derivative having an imidazole moiety, **TTF-Im**, which forms robust H-bond interactions and exhibits simultaneous CT and PT process, was investigated. Our intensive studies revealed the peculiar ability of H-bonds in the control of electronic state and molecular aggregation in CT complexes so as to produce highly conductive CT complexes with various acceptors having a wide range of accepting ability. The robust H-bonds of the imidazole ring in complexes **16**, **21a**, and **22** confirmed the high potential of H-bond interaction in the regulation of molecular arrangements in CT complexes. Furthermore, our study disclosed for the first time that H-bonds between donor and acceptor control the electronic state in the CT complexes: (1) control of the molecular ratio through the site-selective molecular recognition, and (2) redox activation based on the polarizability. These effects of H-bonds controlled the ionicities to give partial CT and highly conductive complexes including metallic CT complex. Furthermore, **TTF-Im** exhibited multiple functions, namely, PT coupled CT process. In the anilic acid complexes **22**−**24**, the strong proton-accepting ability inherent in the imidazole ring system generated the radical dication species, **TTF-Im**$^{\bullet+}$·**H**$^+$. These investigations will provide a new strategy for the molecular design of multifunctional conducting materials and will also highly contribute to the future development of the molecule-based functional materials.

Acknowledgment. This work was partially supported by a Grant-in-Aid for Scientific Research (No. 16350074) from the Ministry of Education, Culture, Sports, Science, and Technology, Japan, by PRESTO-JST, by a grant of The Asahi Glass Foundation, and by the 21COE Program "Creation of Integrated EcoChemistry of Osaka University". T.M. is a recipient of a Japan Society for the Promotion of Science (JSPS) research fellowship.

Supporting Information Available: The procedures of preparation, physical data, electronic and Raman spectra, electrical conductivity, list of selected crystallographic data, selected intramolecular bond lengths and angles of the complexes, variable-temperature IR spectra, and calculated atomic charges (PDF), and crystallographic data (CIF). This material is available free of charge via the Internet at http://pubs.acs.org.

JA072607M